Vol. 25, No. 3(2026) IA26847

Revista Mexicana de Ingeniería Química

UV radiation-induced degradation of E133 dye using a Mn(II) Fenton-like process

Degradación del colorante E133 inducida por radiación UV mediante un proceso tipo Fenton con Mn(II)

H. López-García, C. Romo-Gómez, M. M. Meneses-López, C. Camacho-López*, O. A. Acevedo-Sandoval, J. B. Leyva-Morales

Área Académica de Química, Universidad Autónoma del Estado de Hidalgo, Carretera Pachuca-Tulancingo Km. 4.5, Colonia Carboneras, Mineral de la Reforma, Hidalgo, C.P. 42184.

Received: April 9, 2026; Accepted: June 18, 2026

Abstract

Brilliant Blue dye (E133) is a recalcitrant organic contaminant that is not removed from water by conventional treatment processes. However, the study of photo-Fenton-like processes using catalysts other than iron has emerged as an alternative for its degradation. Therefore, the capacity of Mn^{2+} for E133 degradation through a photo-Fenton-like process was evaluated. Assays were conducted based on a factorial design. The studied factors were pH (4, 7, and 9), E133 (1 and 5 mg L^{-1}), Mn (1 and 5 mg L^{-1}), and H_2O_2 (50 and 150 mg L^{-1}). The highest degradation efficiency and kinetic degradation constant of E133 were 72.68 ± 7.18 % and 8.90 ± 1.97 × 10^{-3} min^{-1}, respectively, obtained at pH 4 with E133 (1 mg L^{-1}), Mn^{2+} (5 mg L^{-1}), and H_2O_2 (150 mg L^{-1}). The use of Mn^{2+} in Fenton-like processes represents a promising alternative for E133 degradation.

Keywords: degradation; E133; photo-Fenton; manganese; advanced oxidation processes.

Resumen

El colorante Azul Brillante (E133) es un contaminante orgánico recalcitrante que no se elimina del agua mediante procesos de tratamiento convencionales. Sin embargo, el estudio de procesos tipo foto-Fenton utilizando catalizadores distintos al hierro ha surgido como una alternativa para su degradación. Por lo tanto, se evaluó la capacidad del Mn^{2+} para la degradación del E133 a través de un proceso tipo foto-Fenton. Los ensayos se realizaron con base en un diseño factorial. Los factores estudiados fueron el pH (4, 7 y 9), el E133 (1 y 5 mg L^{-1}), el Mn (1 y 5 mg L^{-1}) y el H_2O_2 (50 y 150 mg L^{-1}). La mayor eficiencia de degradación y la constante cinética de degradación del E133 fueron 72.68 ± 7.18 % y 8.90 ± 1.97 × 10^{-3} min^{-1}, respectivamente, obtenidas a pH 4 con E133 (1 mg L^{-1}), Mn^{2+} (5 mg L^{-1}) y H_2O_2 (150 mg L^{-1}). El uso de Mn^{2+} en procesos tipo Fenton representa una alternativa prometedora para la degradación del E133.

Palabras clave: degradación; E133; foto-Fenton; manganeso; procesos de oxidación avanzada.

*Corresponding author. *E-mail*: cesar_camacho@uaeh.edu.mx ;
https://doi.org/10.24275/rmiq/IA26847
ISSN:1665-2738, *issn-e*: 2395-8472

1 Introduction

The textile industry is one of the sectors generating the highest global revenues, estimated at up to USD 1 trillion annually. It has even been reported that the sale of textile products contributes approximately 2% to the global gross domestic product (Liu & Wang, 2024). More than 100,000 synthetic organic dyes are currently available on the market, with an annual production reaching up to 1,000,000 tons (Tkaczyk *et al.*, 2020). The continuous use and production of these compounds have been identified as one of the main causes of natural water contamination. Most dyes are composed of aromatic structures, which confer high toxicity and may induce carcinogenic effects in humans and aquatic biota (Sahu & Poler, 2024). The presence of dyes has become one of the major environmental concerns in water due to their persistence, potential toxicity, and ability to disrupt essential ecological processes and human health (Al-Tohamy *et al.*, 2022; Pavithra *et al.*, 2019).

Brilliant Blue (E133) is a synthetic dye belonging to the triphenylmethane auxochrome category and is widely used in the food, textile, and cosmetic industries (Al-Shehri *et al.*, 2021). It has been identified as one of the textile contaminants frequently detected in industrial and municipal effluents. The presence of E133 in the environment alters the visible color of water and reduces solar radiation penetration, thereby affecting photosynthesis and oxygen production in aquatic systems (Negoescu *et al.*, 2021). Furthermore, E133 exhibits high structural stability and resistance to biodegradation due to its conjugated aromatic nature, which promotes its persistence in natural environments and limits the effectiveness of conventional water treatment systems (Drhimer *et al.*, 2023).

Conventional wastewater treatment processes are not designed to biodegrade dyes such as Brilliant Blue, leading to the exploration of alternative removal strategies. Advanced oxidation processes (AOPs) have emerged as promising alternatives for the elimination of recalcitrant compounds such as dyes in water. Among these, Fenton and photo-Fenton processes have demonstrated satisfactory results in the degradation of dyes and certain persistent organic pollutants, such as 17β-estradiol (Guerrero-Martínez *et al.,* 2024, Laverde-Cerda *et al.*, 2020). These systems employ iron-based catalysts to generate hydroxyl radicals (•OH), which act as strong oxidants capable of breaking complex aromatic bonds in organic molecules (Khelassi-Sefaoui *et al.*, 2025). Photo-Fenton processes have attracted considerable attention for the degradation of organic contaminants due to the use of artificial UV or solar radiation as an energy source to accelerate radical formation, thereby improving the oxidative efficiency of the process. However, conventional iron-based Fenton systems are often limited by their requirement for acidic pH conditions and the formation of metallic sludge, which restricts their industrial-scale application (Papadopolou *et al.*, 2025).

The use of transition metals such as manganese (Mn) has emerged as an innovative alternative that reduces the strict operational conditions of conventional Fenton processes due to its redox versatility ($Mn^{2+}/Mn^{3+}/Mn^{4+}$). Mn exhibits high stability and the ability to operate under less restrictive pH conditions, as well as enhancing the formation of reactive oxygen species (Yang *et al.*, 2022). However, its use as the primary catalytic metal remains scarcely explored, as it has mainly been applied in combination with other metaks such as Fe and Cu. In this regard, recent studies have demonstrated the efficient degradation of dyes using Mn-doped nanoparticles and manganese oxides ($Cu_{0.5}Mn_{0.5}Fe_2O_4$), nanocomposites ($MnFe_2O_4$), and photocatalytic configurations activated by solar or UV radiation (Angkaew *et al.*, 2022; Mohammad Hosseini *et al.*, 2025; Wei & Shen, 2022). Therefore, the incorporation of manganese-based catalysts combined with solar radiation offers advantages such as improved energy sustainability, reduced residual sludge generation, adaptability to variable environmental conditions, and a significant reduction in operating costs. Accordingly, the objective of this study was to evaluate the capability of a Mn(II)-based Fenton-like process under UV radiation for the degradation of E133 dye in water. Compared with previous studies, the present work addresses the degradation process of E133 and the effects of varying factors such as pH, Mn concentration, dye concentration, and hydrogen peroxide concentration through a statistical analysis, while minimizing the catalyst concentration as much as possible to obtain environmentally relevant results. Furthermore, this study presents findings regarding the behavior of Mn as the sole catalytic metal in the process.

2 Materials and methods

2.1 Control assays

Control assays were conducted to evaluate potential dye loss due to interaction, volatilization, or photolysis of E133 in the presence of H_2O_2 and Mn^{2+} under UV irradiation and dark conditions. The experimental conditions are summarized in Table 1. The concentrations were fixed at 1 mg L^{-1} of E133 dye, 5 mg L^{-1} of Mn^{2+}, and 150 mg L^{-1} of H_2O_2. All experiments were performed at pH 4, which was adjusted using 0.1 M NaOH or 0.1 M HCl solutions.

Table 1. Experimental design of control assays with (mg L^{-1}) E133 dye (1), Mn^{2+} (5), and H_2O_2 (150) at pH 4 under UV irradiation and dark conditions.

Assay	System	UV irradiation
1	E133	UV irradiation
2	E133 + Mn^{2+}	
3	E133 + H_2O_2	
4	E133 + Mn^{2+} + H_2O_2	
5	E133	Dark conditions
6	E133 + Mn^{2+}	
7	E133 + H_2O_2	
8	E133 + Mn^{2+} + H_2O_2	

Table 2. Factors and levels evaluated in the degradation of E133 dye.

Factors	Levels (mg L^{-1})		
pH*	4	7	9
[E133]		1	5
[Mn]		1	5
[H_2O_2]		50	150

*unitless

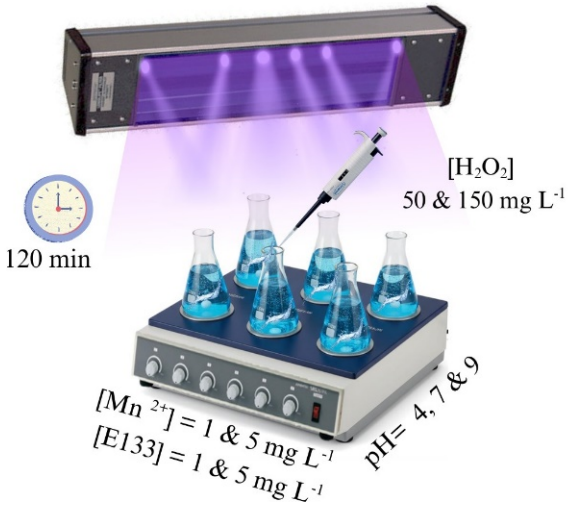

Fig. 1. Schematic representation of the photo-Fenton-like system used for E133 dye degradation experiments.

2.2 E133 degradation assays

The degradation of E133 dye was investigated using a full factorial experimental design. The evaluated factors included pH, Mn^{2+} concentration, H_2O_2 concentration, and initial dye concentration, as shown in Table 2.

The assays were performed in 125 mL Erlenmeyer flasks containing the reaction mixture under continuous magnetic stirring. The supplied UV radiation was maintained constant using a WFH-204B UV lamp emitting at wavelengths of 254 and 365 nm and equipped with a 150 × 50 mm UV filter. The irradiation distance between the lamp and the experimental setup was 28 cm, as illustrated in Fig. 1. All experiments were conducted in duplicate. Liquid samples were collected at 20 min intervals over a total reaction time of 120 min. The collected samples were analyzed immediately without further pretreatment. The pH of the reaction medium was adjusted using 0.1 M NaOH or 0.1 M HCl solutions.

2.3 Analytical methods and evaluated variables

E133 dye concentrations were quantified using a Thermo Scientific GENESYS 10S UV–Vis spectrophotometer at a wavelength (λ) of 629 nm. Calibration curves were prepared in duplicate, yielding coefficients of determination (R^2) greater than 0.99.

The degradation efficiency (E) and degradation rate constant (k) were calculated by fitting concentration data to a pseudo-first-order kinetic model, as expressed in Eqs. (1) and (2), respectively:

$$E\,(\%) = \left(\frac{C_i - C_f}{C_i}\right) * 100 \quad (1)$$

$$\ln\left(C_f\right) = -kt + \ln\left(C_i\right) \quad (2)$$

where C_i, is the initial E133 dye concentration (mg L^{-1}), C_f is the final dye concentration (mg L^{-1}), k is the degradation rate constant (min^{-1}), and t represents reaction time (min).

2.4 Statistical analysis

The normality of degradation efficiency and degradation rate constant data was evaluated using the Shapiro–Wilk test (α = 0.05). The effects of the factors and their levels in the factorial design were subsequently analyzed using analysis of variance (ANOVA). Differences among experimental means were also evaluated by ANOVA (α = 0.05). When statistically significant differences were observed, means were compared using the least significant difference (LSD) test at a significance level of α = 0.05.

3 Results and discussion

3.1 Control assays

The results of the control experiments conducted under dark conditions and UV irradiation are presented in Fig. 2. As shown in Fig. 2a, in systems where only Mn^{2+} or H_2O_2 was individually added, E133 dye concentrations remained nearly constant. Dye concentration losses lower than

10% were estimated. Furthermore, no statistically significant differences were observed among these assays ($p > 0.05$). These results indicate that dye concentration losses due to physical phenomena such as volatilization were negligible. Additionally, no interactions between the dye and the catalyst, such as adsorption processes, were detected.

When Mn^{2+} and H_2O_2 were simultaneously added under dark conditions (Fig. 2a), the dye concentration decreased by 14.83%. These results demonstrate the low reactivity of hydrogen peroxide with Mn for dye degradation in the absence of irradiation. Nevertheless, the system achieved partial E133 removal. Similar findings have been reported, indicating that hydrogen peroxide alone exhibits limited reactivity toward azo and triphenylmethane dyes such as E133 (Bi *et al.*, 2024; Wilayat *et al.*, 2024).

In the systems exposed to UV radiation, dye concentration remained nearly constant in the assays where Mn^{2+} or H_2O_2 was added separately (Fig. 2b). However, when the dye was combined with Mn^{2+} and H_2O_2, a reduction of 73.10% was achieved. These results suggest that UV radiation promoted the activation and formation of •OH radicals, which were catalytically enhanced by Mn, resulting in greater degradation compared with dark conditions. According to Cheng *et al.* (2022) and Meneses-López *et al.* (2026), the possible mechanism for •OH radical generation using Mn (II) as a catalytic metal can be described by Eqs. 3-5:

$$Mn^{2+} + H_2O_2 \rightarrow Mn^{3+} + \bullet OH + OH^- \quad (3)$$

$$H_2O_2 + Mn^{3+} + 2OH^- \rightarrow Mn^{2+} + \bullet O_2^- \quad (4)$$

$$\bullet OH + \bullet O_2^- \rightarrow O_2 + OH^- \quad (5)$$

The presence of Mn in the system facilitated electron capture at active metal sites and simultaneously improved electron transfer, thereby increasing the degradation efficiency of the photo-Fenton-like process (Shafeeyan, 2024).

3.2 Degradation of E133 dye

The degradation efficiencies and degradation rate constants of E133 dye obtained from the factorial design experiments are presented in Table 3. The highest degradation performance was achieved in experiments conducted with E133 (1 mg L^{-1}), H_2O_2 (150 mg L^{-1}), and Mn^{2+} (5 mg L^{-1}) at pH 4, yielding an E133 degradation efficiency of 72.68 ± 7.18% and a degradation rate constant of $8.90 \pm 1.97 \times 10^{-3}$ min^{-1}. The degradation results of E133 were well fitted to a pseudo-first-order kinetic model, with coefficients of determination (R^2) higher than 0.9.

The degradation of organic contaminants such as E133 dye through advanced oxidation processes is a complex phenomenon influenced by several reaction stages, including radical generation rate, mass transfer, radiant energy input, H_2O_2 concentration, and catalyst surface characteristics, among other factors. In this regard, the data obtained from E133 degradation were fitted to a pseudo-first-order kinetics equation through linear regression analysis, yielding coefficients of determination (R^2) higher than 0.95 (Do Nascimento Júnior *et al.*, 2018). Furthermore, the obtained results confirm the ability of Mn^{2+} to accelerate the activation of •OH radicals as well as the formation of other possible reactive oxygen species (ROS) (Y. Liu *et al.*, 2021).

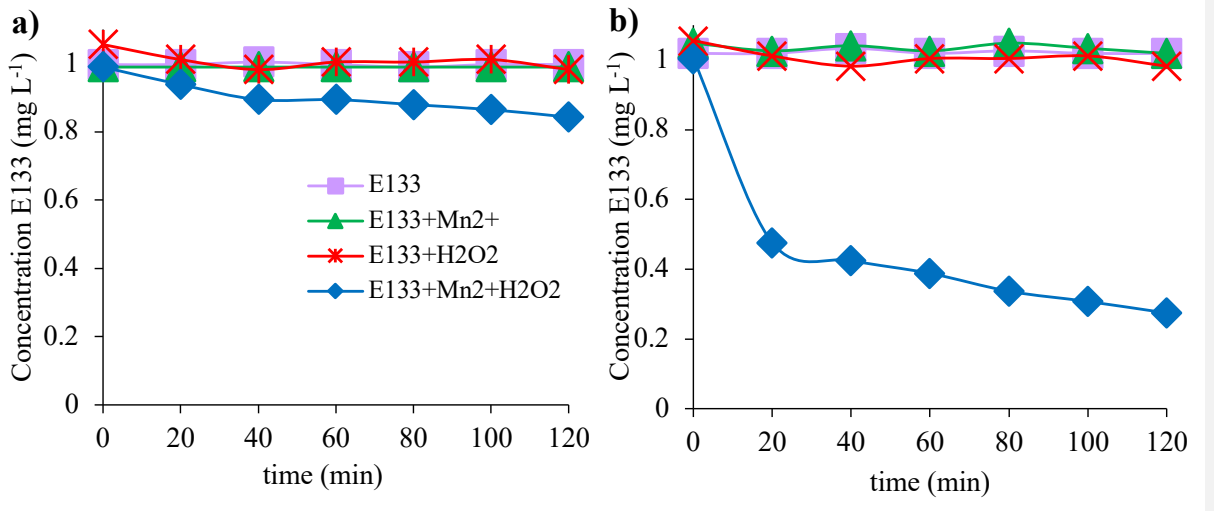

Fig. 2. Kinetic profiles of control assays using 1 mg L^{-1} of E133 dye under (a) dark conditions and (b) UV irradiation.

Table 3. Degradation efficiencies and degradation rate constants obtained from E133 degradation experiments.

pH	E133 (mg L^{-1})	Mn^{2+} (mg L^{-1})	H_2O_2 (mg L^{-1})	Efficiency (%)	Kinetic constant (k) $\times 10^{-3}$ (min^{-1})
4	1	1	50	18.67 ± 2.30	1.60 ± 0.20
			150	66.47 ± 3.75	8.70 ± 1.35
		5	50	31.90 ± 1.72	3.00 ± 0.87
			150	72.68 ± 7.18	8.90 ± 1.97
	5	1	50	36.95 ± 6.34	3.90 ± 0.47
			150	28.95 ± 3.38	2.70 ± 0.29
		5	50	12.85 ± 0.77	1.00 ± 0.29
			150	64.92 ± 1.92	7.80 ± 0.62
7	1	1	50	29.95 ± 3.19	2.30 ± 0.54
			150	51.13 ± 12.40	5.30 ± 1.17
		5	50	48.01 ± 3.93	4.50 ± 1.41
			150	42.84 ± 4.82	3.20 ± 1.51
	5	1	50	31.79 ± 7.91	2.50 ± 0.58
			150	19.59 ± 1.61	1.70 ± 0.40
		5	50	30.30 ± 3.31	3.00 ± 0.24
			150	43.24 ± 1.91	4.30 ± 1.68
9	1	1	50	12.25 ± 5.78	1.30 ± 0.45
			150	47.17 ± 5.49	5.70 ± 0.85
		5	50	4.34 ± 0.47	0.50 ± 0.08
			150	61.97 ± 2.09	7.60 ± 3.1
	5	1	50	32.88 ± 2.65	4.22 ± 0.42
			150	38.05 ± 2.05	4.00 ± 1.25
		5	50	10.59 ± 1.68	1.00 ± 0.34
			150	16.18 ± 9.17	1.6 ± 0.38

Similar results were reported by Yousefi *et al.* (2017), who obtained Brilliant Blue degradation efficiencies ranging from 36.9 to 72.3% using 0.5 g L^{-1} Fe^0 and 1 mM persulfate at pH values between 2 and 6. Likewise, Ganiyu *et al.* (2019) reported E133 degradation efficiencies of 75, 53, 28, and 15% in an electro-Fenton process using applied currents of 50, 100, 250, and 500 mA, respectively, after 60 min of reaction with Fe^{2+} concentrations ranging from 0.1 to 5 mM. These findings demonstrate that the ability of Mn^{2+} to degrade E133 in advanced oxidation processes is comparable to conventional iron-based catalysts used in Fenton systems.

On the other hand, it was observed that reducing the H_2O_2 concentration from 150 to 50 mg L^{-1}, while maintaining 5 mg L^{-1} of Mn^{2+} and increasing the pH to 9, significantly decreased both degradation efficiency and the degradation rate constant. Under these conditions, the lowest degradation efficiencies of the study were obtained, reaching values as low as 4%. These results indicate that increasing the reaction medium pH and reducing hydrogen peroxide concentration negatively affected the degradation performance of the photo-Fenton-like process for E133 dye removal.

The main effects plots obtained from the degradation efficiencies and degradation rate constants derived from the factorial design experiments at different pH values, Mn^{2+} concentrations, H_2O_2 concentrations, and E133 dye concentrations are presented in Fig. 3 and 4, respectively. According to the statistical analysis, the factor that exhibited the greatest influence on degradation efficiency was the variation in H_2O_2 concentration. Increasing the H_2O_2 concentration from 50 to 150 mg L^{-1} resulted in an increase in degradation efficiency from 25.06 to 46.09%. Regarding pH, degradation efficiency increased from 27.91 to 41.70% when the pH was reduced from 9 to 4, with the highest degradation percentages being obtained at pH 4.

3.3 *Effect of Mn^{2+} concentration*

Increasing the Mn^{2+} catalyst concentration from 1 to 5 mg L^{-1} slightly improved the E133 degradation efficiencies, with an increase from 34.51 to 36.65 %. Similarly, the degradation rate constant increased from 3.56 to 3.88 $\times 10^{-3}$ min^{-1} at Mn^{2+} concentrations of 1 and 5 mg L^{-1}, respectively. According to the statistical analysis, catalyst concentration was not a significant factor affecting the evaluated response variables ($p > 0.05$). This represents an advantage of using Mn in Fenton-like processes, since degradation was not dependent on catalyst concentration, at least within the evaluated range of 1–5 mg L^{-1}.

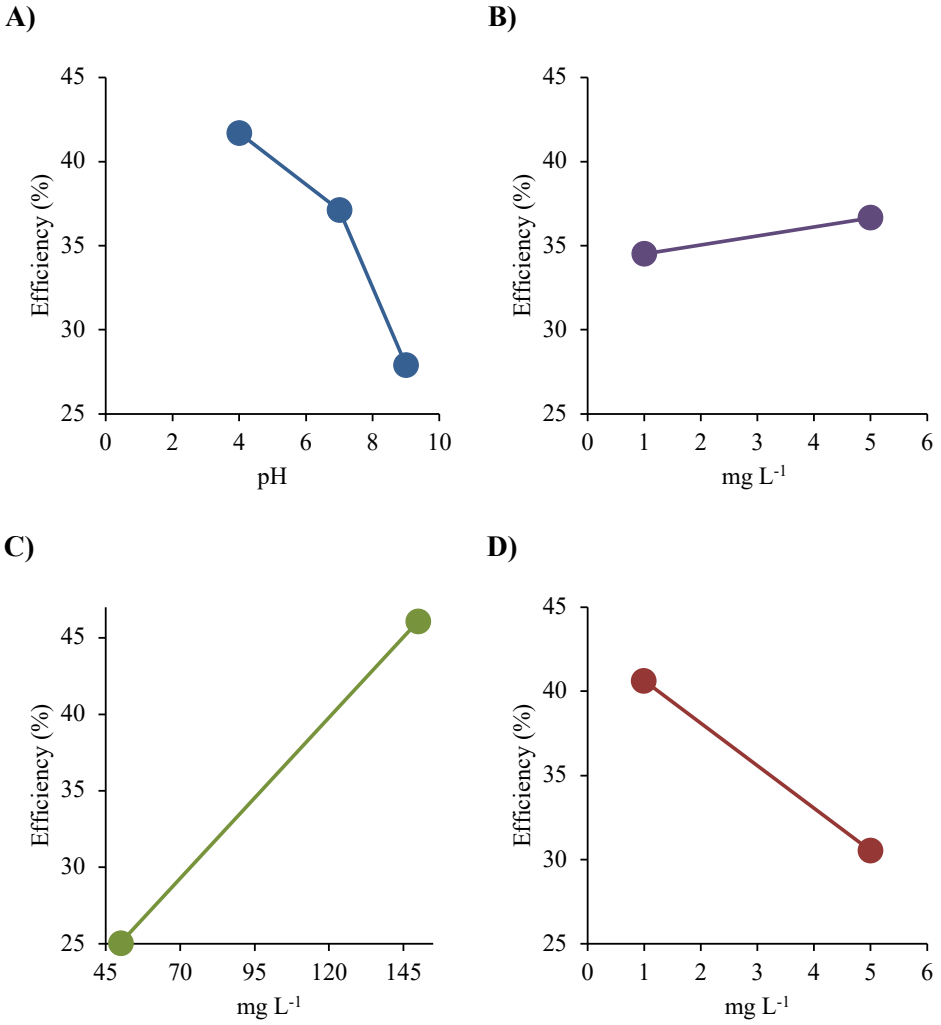

Fig. 3. Main effects plots for E133 dye degradation efficiencies at different values of (A) pH and concentrations of (B) Mn^{2+}, (C) H_2O_2, and (D) E133.

This behavior is associated with the availability of active catalytic sites. During the degradation process, as the dye concentration decreased, a greater availability of catalytic sites became accessible for occupation by contaminant molecules (Yousefi *et al.*, 2017). Therefore, when the Mn^{2+} concentration increased from 1 to 5 mg L^{-1}, a slight increase in degradation efficiency from 34.51 to 36.65% was observed, showing a similar trend for the degradation kinetic constant. The difference between the evaluated catalyst concentration levels was only 4 mg L^{-1}, which may explain the absence of statistically significant changes in the evaluated variables. Nevertheless, it is important to note that excessive increases in catalyst concentration may reduce the effective surface area and consequently promote UV radiation absorption phenomena, thereby decreasing the production of free radicals and directly affecting the E133 degradation process (Jhansi *et al.*, 2025).

Moreover, excessive Mn^{2+} concentrations may lead to accelerated •OH radical production, which can negatively affects E133 degradation because the generated radicals lose energy through secondary reactions within the process (Cheng *et al.*, 2022). Additionally, the catalytic regeneration of manganese can generate hydroxyl radicals through the transfer of trapped holes within the catalytic material, which may have further enhanced dye degradation (Ghosal *et al.*, 2025).

3.4 *Effect of H_2O_2 concentration*

Increasing H_2O_2 concentration from 50 to 150 mg L^{-1} produced a significant improvement in dye degradation efficiency, which increased from 25.06 to 46.09%. Likewise, the degradation rate constant increased from 2.28 to 5.16 × 10^{-3} min^{-1} at H_2O_2 concentrations of 50 and 150 mg L^{-1}, respectively. It is important to mention that the residual H_2O_2 concentration was not quantified, which

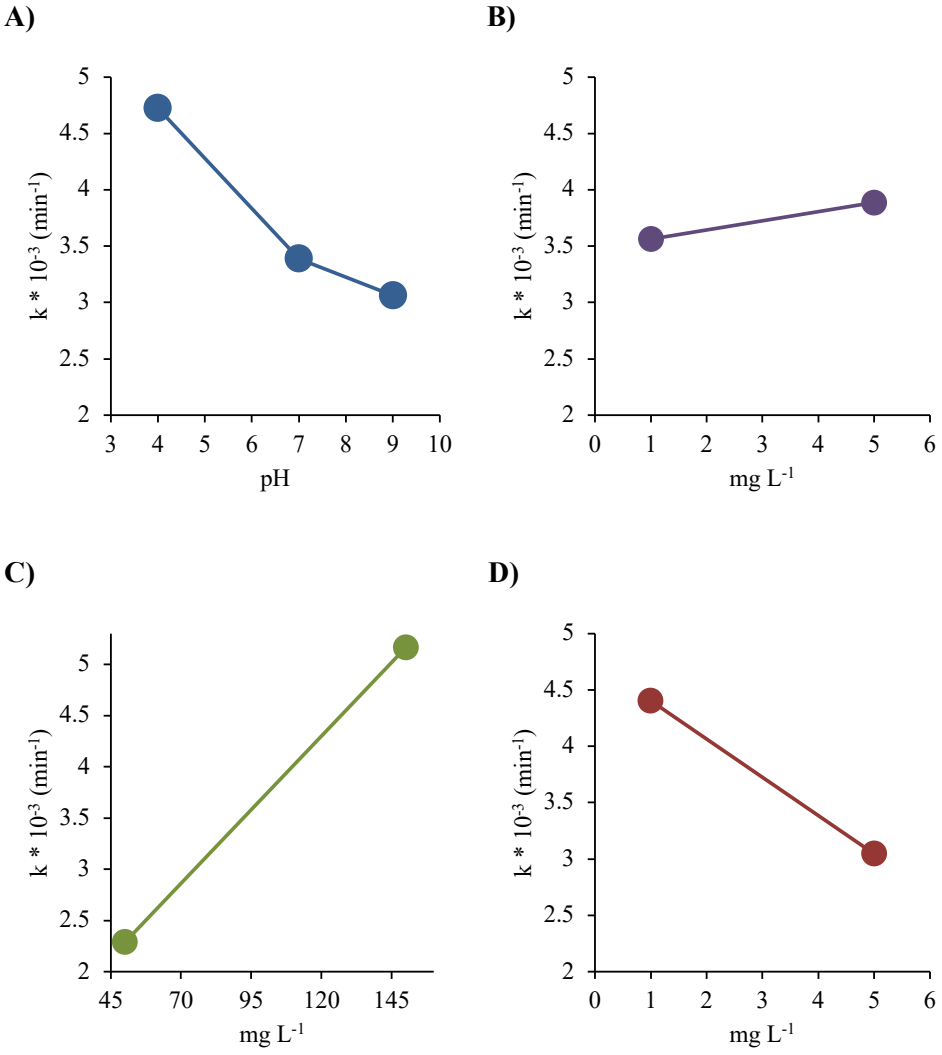

Fig.4. Main effects plots for the kinetic constants obtained from E133 dye degradation assays at different values of A) pH and concentrations of B) Mn^{2+}, C) H_2O_2, and D) E133.

may represent a limitation in the analysis of E133 degradation. Nevertheless, based on the statistical analysis performed, variations in H_2O_2 concentration were identified as the factor that produced the greatest changes in the evaluated response variables ($p < 0.05$). Similar findings were reported by Negoescu *et al.* (2021) during Brilliant Blue degradation experiments in a photo-Fenton system using Brilliant Blue (1×10^{-6} M), Fe^{2+} (1×10^{-3} M), and H_2O_2 ($1–5 \times 10^{-4}$ M).

Since H_2O_2 acts as the oxidizing agent in the system, the primary reactive species generated during the process were hydroxyl radicals (•OH), which exhibit a standard oxidation potential of 2.18 V and reaction rate constants in the range of 10^7 to 10^{10} L mol^{-1} s^{-1}. These characteristics make •OH radicals among the most energetic oxidizing species, thereby enhancing degradation efficiencies in Fenton-like processes (Bury *et al.*, 2025; Zhang *et al.*, 2024).

Furthermore, higher H_2O_2 concentrations increase the distribution of oxidant molecules in the reaction medium, leading to improved •OH radical dispersion. This reduces the diffusion distance between •OH radicals and organic molecules, thereby enhancing degradation performance (Ganiyu *et al.*, 2019).

According to previous reports, the three main degradation pathways of E133 dye mediated by •OH radicals involve hydrogen atom transfer, radical adduct formation, and single-electron transfer mechanisms (Zhang *et al.*, 2024). Similar results were reported by Rayati *et al.* (2024), who observed increased degradation efficiencies of dye mixtures with increasing pH, which was attributed to enhanced •OH radical formation from H_2O_2 decomposition.

3.5 *Effect of E133 concentration*

A decrease in E133 concentration from 5 to 1 mg L^{-1} resulted in an increase in degradation efficiency from 30.52 to 40.63 %.

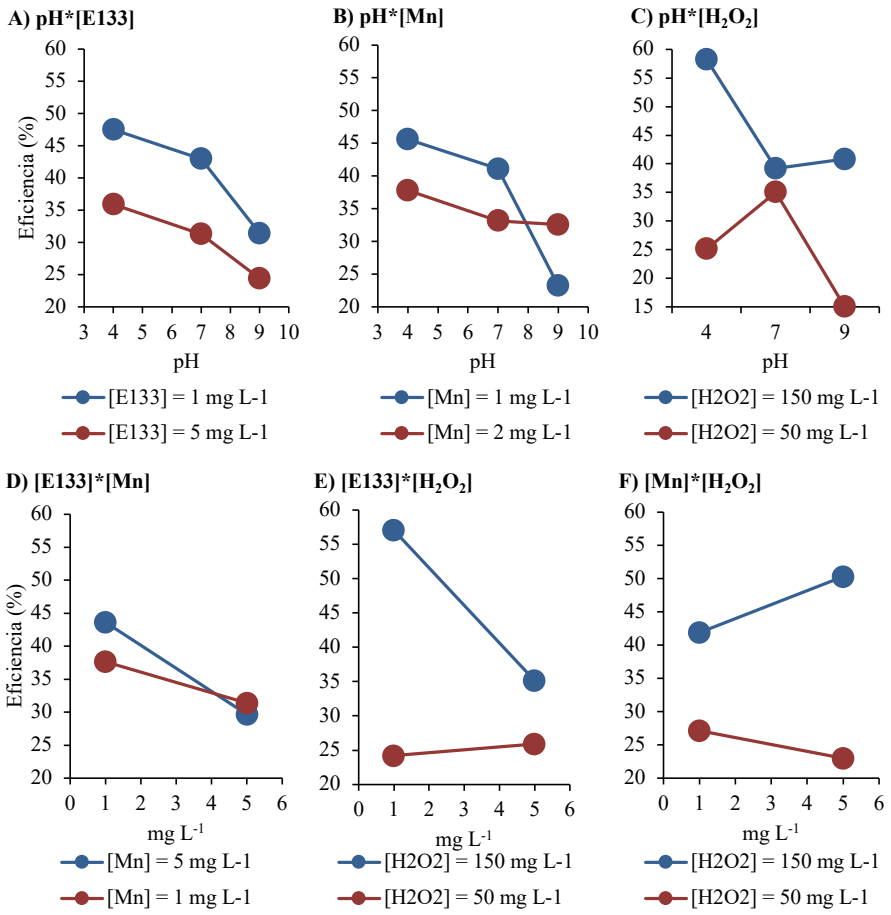

Fig. 5. Interaction plots for degradation efficiencies obtained from E133 dye degradation assays at different values of pH and concentrations of Mn^{2+}, H_2O_2, and E133.

Similarly, the kinetic constant increased from 3.04 to 4.40 × 10^{-3} min^{-1}. Statistical analysis confirmed that dye concentration significantly influenced both response variables ($p < 0.05$).

Higher dye concentrations require a greater availability of •OH radicals, which limits oxidation efficiency and reduces degradation performance (Tu *et al.*, 2022). In addition, elevated dye concentrations may reduce overall process efficiency due to optical shielding and increased radical scavenging caused by substrate excess. Similar behavior has been reported for conventional photo-Fenton systems (Bi *et al.*, 2024; Wilayat *et al.*, 2024).

3.6 *Effect of pH*

Increasing the pH from 4 to 9 reduced degradation efficiency from 41.70 to 27.91 %. Likewise, the kinetic constants decreased from 4.70 to 3.06 × 10^{-3} min^{-1} for assays performed at pH 4 and 9, respectively. Statistical analysis demonstrated that pH significantly affected the evaluated response variables ($p < 0.05$).

The reduction in degradation performance at higher pH values can be attributed to the non-productive decomposition of H_2O_2, which decreases •OH radical generation (Kasetsomboon *et al.*, 2025). Additionally, Mn solubility may decrease as pH increases, reducing catalytic activity and promoting H_2O_2 self-decomposition (Zheng *et al.*, 2024). Manganese catalytic activity is favored under acidic conditions that promote the redox cycling between Mn^{2+} and Mn^{3+}, where Mn^{3+} acts as the active species responsible for H_2O_2 activation and •OH radical formation (Hussain *et al.*, 2021; Riza-Frutos *et al.*, 2023).

3.7 *Interaction between factors*

Interaction plots derived from the factorial design and degradation efficiencies are presented in Figure 5. Statistical analysis revealed significant interactions between pH*[Mn^{2+}], pH*[H_2O_2], [E133]*[H_2O_2], and [Mn^{2+}]*[H_2O_2] ($p < 0.05$). Among these interactions, H_2O_2 concentration was the common factor, which agrees with the results obtained from the statistical analysis and main effects plots shown in Figure 4.

The interaction between pH and H_2O_2 concentration exhibited the strongest influence on degradation efficiency compared with interactions

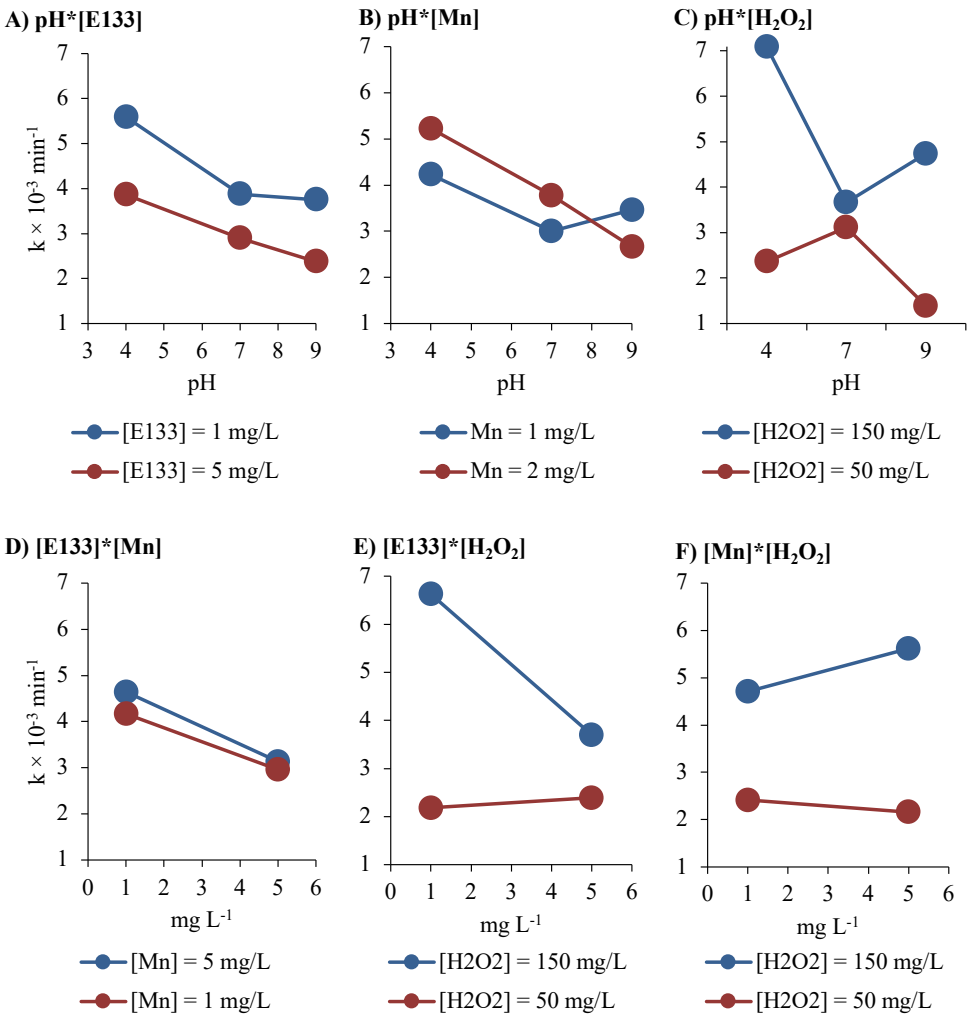

Fig. 6. Interaction plots for the kinetic constants obtained from E133 dye degradation assays at different values of pH and concentrations of Mn^{2+}, H_2O_2, and E133.

involving pH and either E133 or Mn concentrations. The highest degradation efficiencies were achieved under conditions of pH 4, 1 mg L^{-1} Mn^{2+}, 150 mg L^{-1} H_2O_2, and 1 mg L^{-1} E133.

The interaction plots for the kinetic constants are shown in Fig. 6. A similar trend was observed as in the interaction plots for degradation efficiencies (Fig. 5).

According to Jung *et al.* (2009), the stability of •OH radicals in photo-Fenton-like reactions depends on the acidity of the reaction medium, with longer half-lives under acidic conditions. In this context, increasing the pH reduced degradation efficiency, whereas increases in Mn^{2+}, H_2O_2, and dye concentrations enhanced E133 removal. The high degradation efficiencies observed in this study were attributed to the use of Mn^{2+} as the catalyst. Manganese is a transition metal capable of cycling through multiple oxidation states (Mn^{2+}/Mn^{3+}/Mn^{4+}), with Mn^{2+}/Mn^{3+} being the predominant species involved in the degradation process, as shown in Eqs. 4 - 6 (Divya *et al.*, 2026; Hussain *et al.*, 2021).

This represents an advantage compared to Fe^{2+} in conventional Fenton systems, as iron exhibits limited cycling capability. The oxidation of Fe^{2+} to Fe^{3+} has a rate constant of 70 M^{-1} s^{-1}, whereas the reduction of Fe^{3+} to Fe^{2+} occurs at a much slower rate (0.001–0.01 M^{-1} s^{-1}) (González *et al.*, 2020). Despite some H_2O_2 decomposition and the associated reduction in response variables, Mn precipitation was not observed, as E133 concentrations continued to decrease, indicating ongoing generation of reactive oxygen species, primarily •OH (Zheng *et al.*, 2024).

The use of manganese as a catalyst in photo-Fenton-like processes represents a promising alternative for the degradation of organic contaminants such as dyes and structurally similar compounds. Compared to conventional iron-based catalysts, manganese offers greater operational flexibility under diverse environmental conditions. Moreover, the results provide relevant insights into its potential application for real-scale wastewater treatment

processes.

Conclusions

No significant interactions between E133 dye and Mn^{2+} or H_2O_2 were observed under dark conditions or under UV radiation. The highest degradation efficiencies and kinetic constants of E133 were 72.68 ± 7.18 % and 8.90 ± 1.97 × 10^{-3} min^{-1}, respectively, under conditions of 1 mg L^{-1} E133, 150 mg L^{-1} H_2O_2, and 5 mg L^{-1} Mn^{2+} at pH 4. Dye degradation followed a pseudo-first-order kinetic model.

Increasing the pH and the initial E133 concentration reduced the degradation capacity of the photo-Fenton process, whereas higher H_2O_2 and Mn^{2+} concentrations enhanced dye removal. Significant interactions were observed for pH*[Mn^{2+}], pH*[H_2O_2], [E133]*[H_2O_2], and [Mn^{2+}]*[H_2O_2], which exerted the greatest effects on the evaluated response variables. Among all factors, H_2O_2 concentration had the most pronounced influence on E133 photodegradation. The use of Mn^{2+} in a Fenton-like process under UV irradiation proved to be a promising alternative for the degradation of synthetic dyes such as E133, demonstrating results competitive with conventional iron-based catalysts.

The obtained results establish the basis for the use of Mn in the degradation of organic pollutants and its future application in the treatment of real wastewater. Additionally, further studies are required to evaluate the byproducts generated during the E133 degradation process and to compare them with those produced using metals commonly employed in conventional photo-Fenton processes.

References

Al-Shehri, A. S., Zaheer, Z., Alsudairi, A. M. & Kosa, S. A. (2021). Photo-oxidative Decolorization of Brilliant Blue with AgNPs as an Activator in the Presence of $K_2S_2O_8$ and $NaBH_4$. *ACS Omega*, *6*(41), 27510–27526. Doi: https://doi.org/10.1021/acsomega.1c04501

Al-Tohamy, R., Ali, S. S., Li, F., Okasha, K. M., Mahmoud, Y. A., Elsamahy, T., Jiao, H., Fu, Y. & Sun, J. (2022). A critical review on the treatment of dye-containing wastewater: Ecotoxicological and health concerns of textile dyes and possible remediation approaches for environmental safety. *Ecotoxicology and Environmental Safety*, *231*, 113160. Doi https://doi.org/10.1016/j.ecoenv.2021.113160

Angkaew, A., Sakulthaew, C., Nimtim, M., Imman, S., Satapanajaru, T., Suriyachai, N., Kreetachat, T., Comfort, S. & Chokejaroenrat, C. (2022). Enhanced Photo-Fenton activity using magnetic $CU_{0.5}MN_{0.5}FE_2O_4$ nanoparticles as a recoverable catalyst for degrading organic contaminants. *Water*, *14*(22), 3717, doi: https://doi.org/10.3390/w14223717

Bi, W., Du, R., Liu, H., Fu, P. & Li, Z. (2024). Degradation of methyl orange by the Fenton-like reaction of pyrite-activated hydrogen peroxide forming the Fe(III)/Fe(II) cycle. *Water SA*, *50*(2 April). Doi: https://doi.org/10.17159/wsa/2024.v50.i2.4078

Bury, D., Kozera, A. A., Zapaśnik, A., Jakubczak, M., Ściezyńska, D., Bogacki, J., Marcinowski, P., Moszczyńska, D., Prenger, K., Naguib, M. & Jastrzębska, A. M. (2025). Photocatalytic MXenes-magnetite capsules for industrial dye wastewater treatment. *Journal of Alloys and Compounds*, 1041, 183626. Doi: https://doi.org/10.1016/j.jallcom.2025.183626

Cheng, G., Wan, J., Li, Q., Sun, L., Zhang, Y., Li, Z., Dang, C. & Fu, J. (2022). Degradation of reactive brilliant red X-3B by Photo-Fenton-like process: Effects of water chemistry factors and degradation mechanism. *Water*, *14*(3), 380. Doi: https://doi.org/10.3390/w14030380

Divya, V., Anbarasu, K., Vickram, A. & Saravanan, A. (2026). Iron-based nanohybrids for sustainable dye removal from wastewater: A comprehensive review on adsorption mechanisms and environmental implications. *Hybrid Advances*, *12*, 100607. Doi: https://doi.org/10.1016/j.hybadv.2026.100607

Do Nascimento Júnior, W. J., da Rocha, O. R. S., Dantas, Renato F., da Silva, J.P. & Barbosa, A.A. (2018). Kinetic study of food dyes removal from aqueous solutions by solar heterogeneous photocatalysis with artificial neural networks and phytotoxicity assessment. *Desalination and Water Treatment, 104*, 304-314. Doi: https://doi.org/10.5004/dwt.2018.21841

Drhimer, F., Rahmani, M., Regraguy, B., Hajjaji, S. E., Mabrouki, J., Amrane, A., Fourcade, F. & Assadi, A. A. (2023). Treatment of a food industry dye, brilliant blue, at low concentration using a new photocatalytic configuration. *Sustainability*, *15*(7), 5788. Doi: https://doi.org/10.3390/su15075788

Ganiyu, S. O., Brito, L. R., De Araújo Costa, E. C., Santos, E. V. D. & Martínez-Huitle, C. A. (2019). Solar photovoltaic-battery system as a green energy for driven electrochemical wastewater treatment technologies: Application to elimination of Brilliant Blue FCF dye solution. *Journal of Environmental Chemical Engineering*, *7*(1), 102924. Doi: https://doi.org/10.1016/j.jece.2019.102924

Ghosal, P., Gowda, C. C., Chandravanshi, D., Malya, A., Chattopadhyay, K., Kumbhakar, P., Gupta, A. K. & Tiwary, C. S. (2025). Manganese telluride quantum dot decorated 3D printed structures for dye-degradation. *Materials Research Bulletin*, *189*, 113438. Doi: https://doi.org/10.1016/j.materresbull.2025.113438

González, T., Dominguez, J., Cuerda-Correa, E., Correia, S. & Donoso, G. (2019). Selecting and improving activated homogeneous catalytic processes for pollutant removal. Kinetics, mineralization and optimization. *Journal of Environmental Management*, *256*, 109972. Doi: https://doi.org/10.1016/j.jenvman.2019.109972

Guerrero-Martínez, Y. A., Romo-Gómez, C., Camacho-López, C., Acevedo-Sandoval, O. A., González-Ramírez, C. A., Montiel-Palma, S. (2024). HCO3 production from 17β-estradiol oxidation by photo-Fenton as a strategy to avoid the generation of greenhouse gases. *Revista Mexicana de Ingeniería Química, 23*(2), IA24118. Doi: https://doi.org/10.24275/rmiq/IA24118

Hosseini, N. M., Sheshmani, S. & Shahvelayati, A. S. (2025). Manganese ferrite-graphite oxide-chitosan nanocomposite for efficient dye removal from aqueous and textile wastewater under UV and sunlight irradiation. *Scientific Reports*, *15*(1), 866. Doi: https://doi.org/10.1038/s41598-024-84569-9

Hussain, S., Aneggi, E. & Goi, D. (2021). Catalytic activity of metals in heterogeneous Fenton-like oxidation of wastewater contaminants: a review. *Environmental Chemistry Letters*, *19*(3), 2405–2424. Doi: https://doi.org/10.1007/s10311-021-01185-z

Jhansi, K., Pujitha, M., Venkateswarlu, B. & Swaminathan, P. (2025). Evaluation of photocatalytic degradation of rhodamine B using manganese zinc ferrite catalyst. *Next Research.*, *2*(3), 100686. Doi: https://doi.org/10.1016/j.nexres.2025.100686

Jung, Y. S., Lim, W. T., Park, J. & Kim, Y. (2009). Effect of pH on Fenton and Fenton-like oxidation. *Environmental Technology*, *30*(2), 183–190. Doi: https://doi.org/10.1080/09593330802468848

Júnior, W. D. N., Da Rocha, O., Dantas, R. F., Da Silva, J. & Barbosa, A. (2018). Kinetic study of food dyes removal from aqueous solutions by solar heterogeneous photocatalysis with artificial neural networks and phytotoxicity assessment. *Desalination and Water Treatment*, *104*, 304–314. Doi: https://doi.org/10.5004/dwt.2018.21841

Kasetsomboon, N., Pan, W., Zhang, X., Jiang, D., Cao, B., Hu, X., Zheng, A., Wang, S. & Chen, H. (2025). Plasma oxidation via Fenton-like reaction by algae-based activated biochar with Fe sites for dye pollutants degradation in wastewater. *Algal Research*, *92*, 104386. Doi: https://doi.org/10.1016/j.algal.2025.104386

Khelassi-Sefaoui, A., Keniche, A., Khechekhouche, A., Fellah, M., Obrosov, A., El-Hiti, G. A. & Djeziri, S. (2025). Advances in dye degradation in industrial textile effluent: Unveiling the potential of Fenton, photo-Fenton, and helio-photo-Fenton processes for environmental conservation. *Arabian Journal of Chemistry*, 18, 1182025. Doi: https://doi.org/10.25259/ajc_118_2025

Laverde-Cerda, E., Altamirano-Briones, A., Zárate-Pozo, P., Sandoval-Pauker, C., Ramos-Guerrero, L., Muñoz-Bisesti, F., Vargas-Jentzsch, P. (2020). Iron removal for kinetic studies on Fenton treatments: a new approach based on ferrocyanide. *Revista Mexicana de Ingeniería Química, 19*(1), 159-164. Doi: https://doi.org/10.24275/rmiq/Cat545

Liu, X. & Wang, J. (2024). Decolorization and degradation of various dyes and dye-containing wastewater treatment by electron beam radiation technology: An overview. *Chemosphere*, *351*, 141255. Doi: https://doi.org/10.1016/j.chemosphere.2024.141255

Liu, Y., Zhao, Y. & Wang, J. (2021). Fenton/Fenton-like processes with in-situ production of hydrogen peroxide/hydroxyl radical for degradation of emerging contaminants: Advances and prospects. *Journal of Hazardous Materials, 404*, 124191. Doi: https://doi.org/10.1016/j.jhazmat.2020.124191

Meneses-López, M. M., Romo-Gómez, C., Camacho-López, C., Castañeda-Ovando, A.,

Acevedo-Sandoval, O. A., Salas-Martínez, F. (2026). Photodegradation of red 40 via a manganese (II)-based photo-Fenton like process. *Results in Chemistry*, 23, 103177. Doi: https://doi.org/10.1016/j.rechem.2026.103177

Negoescu, D., Oancea, P., Raducan, A. & Puiu, M. (2021). Degradation of Brilliant Blue FCF through photolysis, irradtion and photo-fenton processes: a comparative study. *Revue Roumaine De Chimie*, *66*(3), 281–286. Doi: https://doi.org/10.33224/rrch.2021.66.3.08

Papadopoulou, G., Evgenidou, E. & Lambropoulou, D. (2025). Homogeneous and heterogeneous Photo-Fenton-Based photocatalytic techniques for the degradation of nile blue dye. *Applied Sciences*, *15*(14), 7917. Doi: https://doi.org/10.3390/app15147917

Pavithra, K. G., Kumar, P. S., Jaikumar, V. & Rajan, P. S. (2019). Removal of colorants from wastewater: A review on sources and treatment strategies. *Journal of Industrial and Engineering Chemistry*, *75*, 1–19. Doi: https://doi.org/10.1016/j.jiec.2019.02.011

Rayati, S., Aghajani, S., Nejabat, F. & Nafarieh, P. (2024). Highly efficient oxidative degradation of organic dyes by using magnetically recyclable nanocatalyst based on manganese-porphyrin. *Polyhedron*, *255*, 116961. Doi: https://doi.org/10.1016/j.poly.2024.116961

Riaza-Frutos, A., Egea-Corbacho, A., Manzano, M. A. & Quiroga, J. M. (2023). Oxidation of an Azo-Dye via the Photo-Fenton Process under Heterogeneous and Homogeneous Conditions. *Water*, *15*(9), 1787. Doi: https://doi.org/10.3390/w15091787

Sahu, A. & Poler, J. C. (2024). Removal and degradation of dyes from textile industry wastewater: Benchmarking recent advancements, toxicity assessment and cost analysis of treatment processes. *Journal of Environmental Chemical Engineering*, *12*(5), 113754. Doi: https://doi.org/10.1016/j.jece.2024.113754

Shafeeyan, M. S. (2024). Application of photocatalytic and fenton processes for the degradation of toxic pollutants from pulp and paper industry effluents. *Water Resources and Industry*, *32*, 100260. Doi: https://doi.org/10.1016/j.wri.2024.100260

Tkaczyk, A., Mitrowska, K. & Posyniak, A. (2020). Synthetic organic dyes as contaminants of the aquatic environment and their implications for ecosystems: A review. *The Science of the Total Environment*, *717*, 137222. Doi: https://doi.org/10.1016/j.scitotenv.2020.137222

Tu, Y., Shao, G., Zhang, W., Chen, J., Qu, Y., Zhang, F., Tian, S., Zhou, Z. & Ren, Z. (2022). The degradation of printing and dyeing wastewater by manganese-based catalysts. *The Science of the Total Environment*, *828*, 154390. Doi: https://doi.org/10.1016/j.scitotenv.2022.154390

Wei, J. & Shen, W. (2022). FeOOH quantum dot decorated flower-like WO3 microspheres for visible light driven photo-Fenton degradation of methylene blue and acid red-18. *Colloids and Surfaces a Physicochemical and Engineering Aspects*, *643*, 128754. Doi: https://doi.org/10.1016/j.colsurfa.2022.128754

Wilayat, S., Fazil, P., Khan, J. A., Zada, A., Shah, M. I. A., Al-Anazi, A., Shah, N. S., Han, C. & Ateeq, M. (2024). Degradation of malachite green by UV/H2O2 and UV/H2O2/Fe2+ processes: kinetics and mechanism. *Frontiers in Chemistry*, *12*, 1467438. Doi: https://doi.org/10.3389/fchem.2024.1467438

Yang, Z., Shan, C., Pignatello, J. J. & Pan, B. (2022). Mn(II) Acceleration of the Picolinic Acid-Assisted Fenton Reaction: New Insight into the Role of Manganese in Homogeneous Fenton AOPs. *Environmental Science & Technology*, *56*(10), 6621–6630. Doi: https://doi.org/10.1021/acs.est.1c08796

Yousefi, M., Ghanbari, F., Zazouli, M. A. & Madihi-Bidgoli, S. (2017). Brilliant Blue FCF degradation by persulfate/zero valent iron: the effects of influencing parameters and anions. *Desalination and Water Treatment*, *70*, 364–371. Doi: https://doi.org/10.5004/dwt.2017.20478

Zhang, C., Ding, N., Pan, Y., Fu, L. & Zhang, Y. (2024). The degradation pathways of contaminants by reactive oxygen species generated in the Fenton/Fenton-like systems. *Chinese Chemical Letters*, *35*(10), 109579. Doi: https://doi.org/10.1016/j.cclet.2024.109579

Zheng, J., Lim, H. J., Hedtke, T., Kim, J. & Zhang, S. (2024). Manganese oxide for heterogeneous Fenton treatment: Catalyst or inhibitor? *Applied Catalysis B: Environmental*, *359*, 124531. Doi: https://doi.org/10.1016/j.apcatb.2024.124531